

# Self-Assembly of Flat Micro Components by Capillary Forces and Shape Recognition

J. Fang, S. Liang, K. Wang, X. Xiong, K. F. Böhringer\*

This paper summarizes our recent reports on self-assembly of flat micro components based on two major mechanisms: capillary-driven self-assembly and feature-directed self-assembly. The capillary-driven self-assembly is demonstrated in both a liquid environment and an air environment, and high accuracy self-alignment is achieved due to interfacial energy minimization. Working devices such as Light Emitting Diode (LED) and PZT components are successfully assembled by the capillary-driven self-assembly processes. The feature-directed self-assembly relies on complementary features on micro components and receptor sites, thereby has no constraint on component shapes. Two different feature-directed and uniquely orienting self-assembly processes are demonstrated: one is a semi dry process based on gravity-driven self-alignment, and the other is a completely dry process based on two-stage shape recognition. The feature-directed and uniquely orienting self-assembly processes can be applied to either wafer level packaging of micro devices or part feeding and palletizing for robotic assembly systems.

## 1. Introduction

To build complex microelectromechanical systems (MEMS), monolithic fabrication is often challenged by process and material incompatibilities. Usually MEMS are built as hybrid systems by integrating of components of different types and substrates: components of each type are monolithically fabricated at the highest spatial density on a substrate, and then the substrate is diced into individual parts, finally these different types of components are integrated to construct the hybrid MEMS. The integrating process requires accurate placement of all the micro components, which can be achieved with micro assembly techniques.

Packaging of a typical micro device has two major goals: (1) closely packed interconnect pads on the device chip are redistributed to a larger and manageable area so that input and output leads can be easily attached to the interconnect pads; (2) the device chip is encapsulated in a protective body, and heat dissipation should be taken into account for chips having heat generation and temperature sensitivity. Usually a micro chip is assembled to a chip carrier via flip-chip bonding, which requires the chip to be accurately positioned with correct face and in-plane orientations: the face having interconnect pads touches the chip carrier and the polarity of the chip is matched to that of the receptor site. To package micro device chips correctly, micro assembly techniques are also needed.

Current micro assembly techniques include robotic assembly and self-assembly

---

\* Department of Electrical Engineering, University of Washington, Seattle, WA 98195-2500  
Email: {jdfang, popobear, kerwin, rxiong, karl}@ee.washington.edu

by several different mechanisms. A typical robotic assembly process has three major steps: feed parts with correct orientations; pick and place parts; fix parts in receptor sites. The serial robotic pick-and-place process has several limitations: (1) it is a serial process challenged by mass packaging of large numbers of parts such as RFID chips; (2) it is difficult to release micro parts from micro manipulators because adhesive forces dominate gravitational forces; (3) parts with rotational symmetries are very challenging for part feeding to obtain unique in-plane orientation. Self-assembly techniques enable mass packaging and integrating of micro devices at practical time frames. Current self-assembly techniques for meso scale flat parts are based on two major mechanisms: capillary-driven self-assembly and shape-directed self-assembly.

Several other research groups have developed capillary-driven self-assembly processes in water environments: melting solder [1] or acrylate-based adhesive liquid [2] droplets on receptor sites attract and align parts by minimizing interfacial energies. The solder-driven self-assembly process can select the unique Au bonding face of a component due to the high wetting selectivity of melting solder on Au versus many other surfaces, but this process also has several limitations such as: (1) low melting point of solder limits operating temperatures of assembled devices; (2) each receptor site has only one melting solder droplet, which indicates the number of electrical interconnections between the assembled device and the device carrier substrate is limited to one; (3) parts with rotational symmetries can not be uniquely aligned.

Shape-directed self-assembly is another promising assembly technique for micro components. In 1994 Yeh and coworkers developed a fluidic self-assembly process [3]: trapezoidal components are transported by water flow on a surface with complementary trapezoidal wells until they fall and fit into the wells. This self-assembly process is based on shape recognition between outline of components and receptor sites, which indicates no unique in-plane orientation can be achieved for components with rotational symmetries such as rectangular or square components.

Our research on both capillary-driven self-assembly and shape-directed self-assembly includes the following aspects: (1) controlled multi batch self-assembly by capillary forces [4]; (2) unique alignment of components with special shapes by capillary forces [5]; (3) strong mechanical bonding for actuating components [6]; (4) unique alignment of components having arbitrary shapes based on feature matching instead of outline shape matching [7]; (5) completely dry assembly for components with either movable micro structures or coatings sensitive to aqueous environments [8].

We organize the remaining sections as follows: Section 2 introduces working principles for capillary-driven self-assembly and feature-directed self-assembly; Section 3 discusses the capillary-driven self-assembly processes respectively in a water environment and an air environment; Section 4 presents the feature-directed self-assembly processes: a semi dry assembly process and a completely dry assembly process; Section 5 gives conclusions and discussions.

## **2. Working Principles of Self-Assembly**

### **2.1 The Capillary-Driven Self-Assembly**

Here we discuss two types of capillary-driven self-assembly processes: one in air and the other in water (Fig. 1). Receptor sites for an in-air process are hydrophilic with hydrophobic thiolated Au background (a hydrophobic alkanethiol self-assembled

monolayer, abbreviated as SAM, is chemically bonded to a clean Au surface), while receptor sites for an in-water process are hydrophobic thiolated Au with hydrophilic SiO<sub>2</sub> background.

In both in-water and in-air cases, adhesive liquid (we use an acrylate-based adhesive for polymerization after assembly) wets exclusively the receptor sites, which can be reasoned as follows: in the in-water case, SAM-adhesive and SiO<sub>2</sub>-adhesive interfacial energies are less than 1 mJ/m<sup>2</sup> and much lower than SAM-water interfacial energy of 46 mJ/m<sup>2</sup> [9], so adhesive favors the SAM coated receptor sites; in the in-air case, hydrophilic receptor sites have more attraction to adhesive than the hydrophobic background.

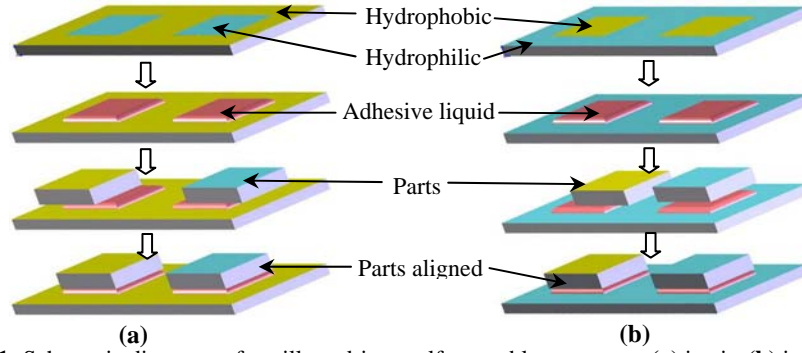


**Fig. 1:** Schematic diagrams of capillary-driven self-assembly processes: (a) in air; (b) in water.

When parts are introduced onto adhesive droplets on receptor sites, either hydrophobic or hydrophilic faces of the parts can be attracted to the adhesive droplets (for each part in the illustration of Fig. 1, one side is hydrophobic and the other side is hydrophilic). This attraction is due to interfacial energy minimization, which is explained as follows: assuming an adhesive droplet forming a thin, flat film such that sidewall interfacial energy of the adhesive can be ignored, the interfacial energies for a part away from and in touch with an adhesive droplet can respectively be approximated with:

$$E_1 = \gamma_{am} |R| + \gamma_{pm} |R| \quad (\text{Eq. 1})$$

$$\begin{aligned} E_2 &= \gamma_{am} (|R| - |P \cap R|) + \gamma_{pm} (|P| - |P \cap R|) + \gamma_{ap} |P \cap R| \\ &= E_1 + (\gamma_{ap} - \gamma_{am} - \gamma_{pm}) |P \cap R| \\ &= E_1 + \Delta E \end{aligned} \quad (\text{Eq. 2})$$

Where  $\gamma_{ij}$  is interfacial energy between surface  $i$  and  $j$ ; subscripts  $a$ ,  $m$  and  $p$  are respectively adhesive, environment medium (water or air) and part surface in contact with adhesive; usually part  $P$  and receptor site  $R$  are mirror images of each other;  $|A|$  indicates the area of surface  $A$ . For an adhesive droplet sitting on a part surface  $P$  with a contact angle  $\alpha$ , Young's equation gives the following relationship:

$$\gamma_{am} \cos(\alpha) + \gamma_{ap} = \gamma_{pm} \quad (\text{Eq. 3})$$

From Eq. 3, we can easily get:

$$\gamma_{ap} - \gamma_{am} - \gamma_{pm} = -\gamma_{am} [\cos(\alpha) + 1] \quad \forall \alpha \in (0^\circ, 180^\circ) \quad (\text{Eq. 4})$$

Eq. 4 indicates that  $\Delta E$  is less than zero for any adhesive, part surface and environment medium. So no matter whether in water or air, a part tends to be in contact with adhesive by its hydrophobic or hydrophilic surface for a lower interfacial energy. Then from Eq. 2, we can see that the interfacial energy has a minimum value when the part is exactly aligned with the receptor site. The alignment accuracy can reach sub microns [2].

## 2.2 The Feature-Directed Self-Assembly

We have developed two different feature-directed and uniquely orienting self-assembly processes. One of the feature-directed self-assembly processes is based on the peg-in-hole mechanism and gravity-driven self-alignment (Fig. 2a). Each part has a circular peg (CP) offset from its center of mass, and each receptor site on an alignment template (ALT) has a circular trench (CT). The assembly completes in two steps: (1) parts are anchored to receptor sites in one-to-one mode; (2) gravity drives all the anchored parts to align with receptor sites when the ALT is tilted in an appropriate orientation, and at the same time free redundant parts slide away. Due to gravity, all the parts are uniquely aligned to the same orientation. The other feature-directed self-assembly process relies on a mechanism of two-stage shape recognition (Fig. 2b). Each part has a CP offset from the center of mass and a cross peg (XP), and correspondingly each receptor site has a CT and a cross trench (XT). The height of the CP is twice that of the XP. The CT and XT mate exclusively their counterpart CP and XP, respectively. The assembly process is two-stage shape recognition: each part is first anchored to a receptor site when its CP falls into a CT (1st shape recognition), and then the anchored part rotates about the CP until its XP fits into the XT (2nd shape recognition). On the same ALT, each assembled part can have different in-plane orientation. The feature-directed self-assembly has a big advantage over outline-shape-directed self-assembly: it has no constraint on the part shape. For simplicity in later reference, we name the above two feature-directed self-assembly processes respectively as single- and double-peg-directed self-assembly process.

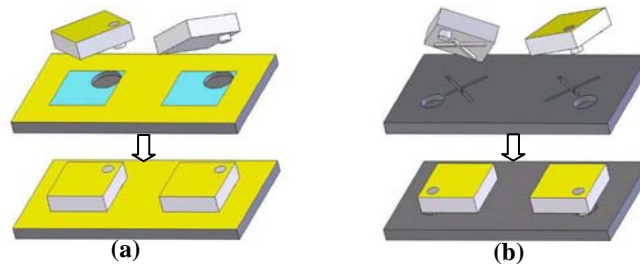


**Fig. 2:** Schematic diagrams of feature-directed self-assembly: **(a)** each part having a single circular peg uniquely aligned with its receptor site having a circular trench; **(b)** each part having a circular peg and a cross peg uniquely aligned with its receptor site having a circular trench and a cross trench.

## 2.3 Major Steps of Self-Assembly Processes

A typical self-assembly process is aiming to organize randomly oriented bulk

parts on a substrate in an array and with desired in-plane orientations. Given bulk parts and an ALT having an array of receptor sites, self-assembly can be achieved with three major steps: (1) parts introduced to receptor sites (feeding); (2) parts aligned to receptor sites (aligning); (3) parts mechanically and/or electrically bonded to the ALT or another substrate (bonding). As the first step, part feeding should satisfy two requirements for proper assembly of most types of components: (1) each receptor site is allocated to only one part; (2) each receptor site sees the bonding face of the introduced part. Unique alignment is required for a part with polarity such as surface mounted LED components. The previous two subsections described only aligning strategies; we will discuss the three steps for each self-assembly process comprehensively in the next two sections.

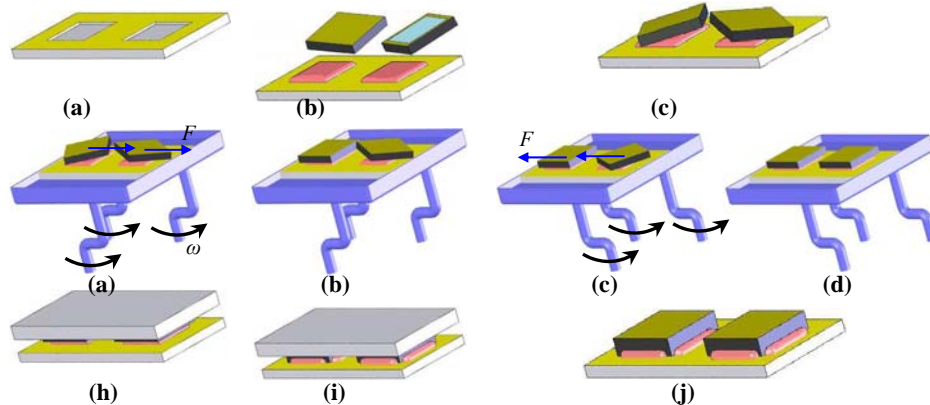


**Fig. 3:** Schematic diagrams of capillary-driven self-assembly of PZT actuators in air: (a) a hydrophobic substrate with two hydrophilic recessed receptor sites; (b) top and bottom views of a PZT actuator, and receptor sites exclusively wetted by adhesive liquid; (c) PZT actuators roughly placed on adhesive droplets with hydrophilic bonding faces downward; (d) the left tilted PZT temporarily balanced by a right-pointing centrifugal force from orbital shaking; (e) the left PZT aligned; (f) the right tilted PZT temporarily balanced by a left-pointing centrifugal force; (g) the right PZT aligned; (h) a pressing plate introduced onto the aligned PZT array; (i) excessive adhesive liquid squeezed out, thereby the rims of PZT actuators directly contact the substrate to achieve electrical connections; (j) adhesive polymerized by heat; (k) the pressing plate removed and top electrodes established with wire bonding.

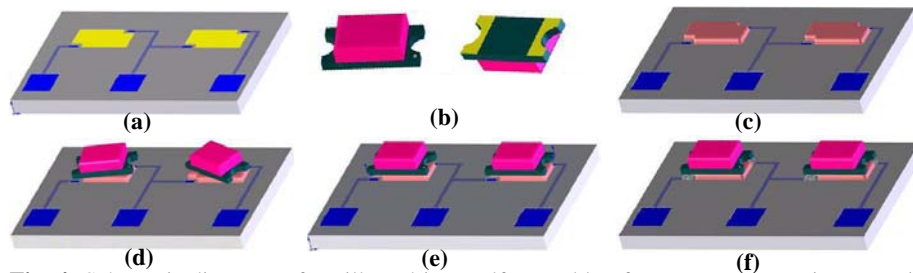


**Fig. 4:** Schematic diagrams of capillary-driven self-assembly of LED components in water: (a) an assembly substrate patterned with hydrophobic receptor sites; (b) top and bottom views of a LED component; (c) receptor sites wetted by adhesive liquid in a water environment; (d) LED components roughly placed onto adhesive droplets; (e) LED components aligned to receptor sites and adhesive polymerized by heat; (f) electrical connections established by electroplating.

### 3. The capillary-driven self-assembly processes

We have applied in-air and in-water capillary-driven self-assembly processes to assemble PZT actuators and LED components, respectively. The schematic diagrams of the complete assembly processes are respectively shown in Fig. 3 and 4.

#### 3.1 Part Feeding

The degree of difficulty to meet the two requirements of part feeding (in Section 2.3) depends on the type of adhesive liquid used on receptor sites. Melting solder has very few well-wetting surfaces such as Au and Cu which can be used as the unique bonding face for a part, and melting solder has very high surface tension which leads to very quick alignment of a captured part, thereby both feeding requirements can be easily satisfied. The acrylate-based adhesive we use for both LEDs and PZTs assembly can wet most surfaces including hydrophilic surfaces and hydrophobic surfaces, so that it can attract a randomly fed part either by its bonding face or other faces. In our previous experiments, we manually introduced PZT and LED components near receptor sites of a stationary substrate to satisfy both of the feeding requirements. According to Eqs. 2 and 4, the strength of attraction between adhesive and a part face depends on the hydrophilicity of the face, so appropriate agitation applied to the assembly substrate can possibly de-bond parts attracted by wrong faces.

During an in-air capillary-driven self-assembly process, we have successfully obtained one-to-one registration of parts onto receptor sites [10]. The experimental setup is schematically shown in Fig. 5a: water droplets wet an array of hydrophilic receptor sites on a downward facing hydrophobic substrate, and dummy silicon parts are agitated by the vibrating diaphragm of an activated speaker to jump randomly. Once a part touches a water droplet, it is immediately captured by the receptor site because water surface tension is much greater than part gravity. An assembly result is shown in Fig. 5b. The assembly rate and yield ratios rise with vibrating amplitude of the diaphragm and part redundancy.

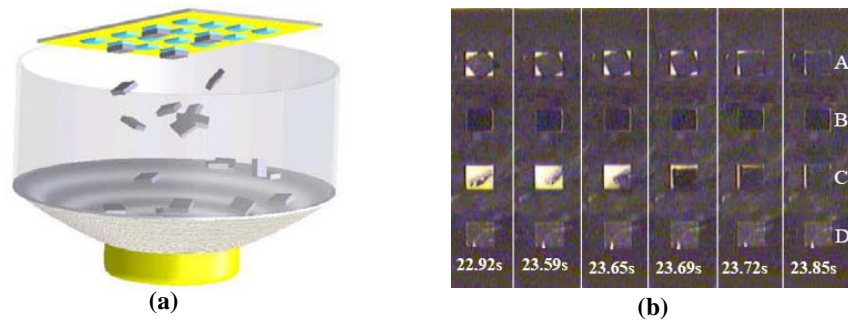


**Fig. 5:** (a) Schematic diagram of the experimental setup for part feeding with an agitated diaphragm. (b) video frames of a column of receptor sites during an assembly experiment (a CCD camera is mounted to see the backside of the glass substrate and the opaque area is hydrophobic thiolated Au): on receptor site A, the part is driven to self-align by capillary force; on receptor site B and D, parts are already aligned; on receptor site C, a part vertically attached is impacted by another jumping part and becomes correctly aligned.

### 3.2 Part Aligning

Capillary-driven self-alignment is based on interfacial energy minimization. When a part is captured by an adhesive droplet on a receptor site in either water or air, the total interfacial energy is approximately linear with overlap area between the part and receptor site [9]. The overlap area maxima at exactly aligned states correspond to interfacial energy minima. For simplicity, if a part is considered to rotate about the geometrical center of a receptor site, then we can easily find that the number of aligned states is proportional to the number of rotational symmetries: square and rectangular parts have respectively four and two preferred orientations, and a circular part has infinity possible aligned states.

Whether a part with rotational symmetries should be uniquely aligned depends on the type of the part. A PZT actuator has only two electrodes - top and bottom complete surfaces, therefore it requires no alignment uniqueness to guarantee correct electrical connections to the substrate. LED components can be turned on only when they are forward biased, so they should be uniquely aligned to obtain correct electrical connections to the substrate having a control circuit for the LED components: randomness among multiple aligned states is definitely a disaster for the control circuit to function as expected.

Unique alignment is usually required for most components to achieve correct electrical connections to an assembly substrate. The capillary-driven self-alignment mechanism indicates that unique alignment can only be achieved for asymmetrical parts. We have successfully obtained unique alignment of offset ring parts (Fig. 6) [5].

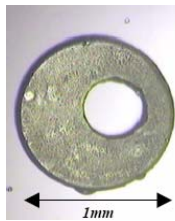


**Fig. 6:** A silicon part in offset ring shape is uniquely aligned during an in-water capillary-driven self-assembly process.

### 3.3 Part Bonding

For the PZT and LED assembly, we used acrylate-based adhesive as the medium, which can be polymerized in about half an hour at 80°C. Permanent bonding is achieved with this polymerized adhesive. It provides only mechanical bonding because it is not electrically conductive.

To establish electrical connections between assembled parts and the substrate, electroplating is one choice. For the LED assembly, each rectangular receptor site sacrifices two small spaces respectively near two diagonal corners for electroplating seeds: patterned Cr/Ni is used as the electroplating seeds, which are hydrophilic without being covered by adhesive liquid in water. Other than the areas for electroplating seeds and contacting pads, Cr/Ni is covered with a passivation layer such as spin-on-glass (SOG) and sputtered nitride.



**Fig. 7:** 28 PZT actuators self-assembled on a 4-inch pump substrate.

Given properly recessed receptor sites, a pressing plate method can also produce electrical connections for components assembled with non-conductive adhesive. For the PZT assembly, each receptor site is recessed by 24  $\mu\text{m}$  in depth and equal in size to the central hydrophilic nickel area on the bonding face of a PZT actuator, and excess adhesive under aligned PZTs is squeezed out by a pressing plate so that each PZT directly contacts the substrate. Mechanical and electrical connections are respectively established at the central and rim areas of PZT actuators. In addition, the pressing plate method brings several other advantages for assembled components: (1) assembled parts sit flat on the assembly substrate; (2) adhesive thickness is accurately controlled by etching methods to recess receptor sites. Conventionally PZT actuators are manually glued with highly viscous silver epoxy, which is a serial process without good control of parameters such as placement, flattening and adhesive thickness. The in-air capillary-driven self-assembly makes the PZT assembly process highly repeatable. An array of PZT assembled for micro pumps on a 4-inch substrate is shown in Fig. 7.

A de-bonding test is performed to compare the strength of bonding by in-air and in-water capillary-driven self-assembly processes. For the in-air process, each PZT having 3mm square bonding area is assembled on a hydrophilic receptor site; for the in-water process, each 3mm square PZT is assembled on a hydrophobic thiolated Au receptor site. In both cases, PZTs are permanently bonded with polymerized acrylate-based adhesive. A shear force applied to one edge of the PZT is increased until the PZT is de-bonded or damaged. The experiment results show that the PZT assembled by the in-water process is de-bonded at a shear stress of about  $8.89 \times 10^5$  Pa, while a shear stress of about  $2.22 \times 10^6$  Pa breaks the PZT assembled by the in-air process rather than the bonding. The de-bonding of the PZT assembled by the in-water process takes place at the interface between the adhesive and the thiolated Au receptor site. Actuating elements such as PZT actuators require strong mechanical bonding, so the in-air self-assembly process is a better choice to assemble actuators than the in-water self-assembly process.

### 3.4 Multi-batch Assembly

We have developed an electrochemical process to desorb SAMs on Au surfaces [4], which enables multi-batch capillary-driven assembly in water. An Au surface is hydrophilic when clean and becomes hydrophobic after adsorbing a SAM. For the in-water capillary-driven self-assembly, the Au receptor site is active only when it is covered with hydrophobic SAM. Reductive desorption of SAMs on an Au surface such as the receptor site can be achieved in a conventional three-electrode electrochemical cell [11], with the Au surface as the working electrode, a platinum mesh as the counter electrode, and a saturated calomel electrode (SCE, Accumet) as the reference electrode. Receptor sites can be turned into an inactive or active state by using a SAM desorption

or adsorption process for different assembly batches.

## 4. The Feature-Directed Self-Assembly Processes

The mechanisms for alignment uniqueness of both the single- and double-peg-directed self-assembly processes have been demonstrated in Section 2.2. Some appropriate part feeding techniques are required to prepare parts for unique self-aligning. We have developed two different feeding techniques, and both of them satisfy the two requirements of part feeding (in Section 2.3). Dummy silicon parts are used for the following proof-of-concept demonstrations.

### 4.1 Part Feeding

#### Method I (*a wet process*)

2mm square silicon parts with a single peg are used for this demonstration. Each silicon part is coated with Au on the face opposite to the peg, and then soaked in a Nanostrip solution to oxidize the silicon surface, and finally soaked in a 1mmol alkanethiol solution to form a hydrophobic SAM on the Au surface. After all the treatments, each part has a unique hydrophobic Au face, while all the other faces are hydrophilic silicon oxide.

The first step is to uniquely face-orient bulk parts. Initially we submerge bulk parts in water in a beaker attached to an orbital shaker. When the orbital shaker runs, the water surface becomes a tilted plane and greater shaking speeds produce higher slopes (Fig. 8). Orbital shaking above a critical speed causes some parts at the beaker bottom to be exposed to air, and then water surface tension drags and floats these parts. On this agitated water surface, only parts with hydrophobic faces in air stay floating, which is their only stable state. In addition, all the floating parts stay neighboring each other in a single layer.

The second step is to palletize the floating parts onto an ALT. A 3-inch pyrex wafer is coated with transparent hydrophobic fluorocarbon polymer PFC802 (Cytonix Co.) on one side and used as a carrier wafer (CWF) to transfer parts. When the CWF is vertically inserted into water, the water surface curves downwards near the hydrophobic PFC802 surface, so that floating parts are attracted to the PFC802 surface by minimizing potential energies. When the CWF continues to enter the water, floating parts start to adhere firmly to the PFC802 surface. After all floating parts adhere to the CWF, the CWF is withdrawn from the water. From our experience, more than 98% of parts stayed on the CWF due to surface tension by water residue. Finally the CWF is turned over an ALT, and all parts are released to the ALT when the water evaporates by heating. As a result, the parts are palletized with their pegs touching the ALT surface.

The final step is to distribute parts to receptor sites. The ALT is attached onto the platform of an orbital shaker. Centrifugal force from orbital shaking drives parts to move randomly until they are anchored to receptor site CTs. The CTs have greater diameters than the CPs of parts for easier trapping. To guarantee one-to-one registration of parts, we should limit the CT diameter so that one CT can only accommodate one CP. We obtained 95% - 99% trapping yields in 3 minutes with 0 - 30% part redundancy (Fig. 9) on a 4-inch ALT having 164 receptor sites (Fig. 10).

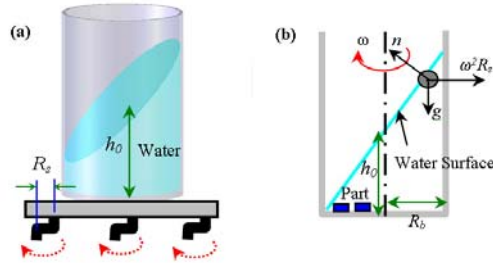


**Fig. 8:** (a) Tilted water surface by orbital shaking; (b) Force analysis of an element on the tilted water surface.

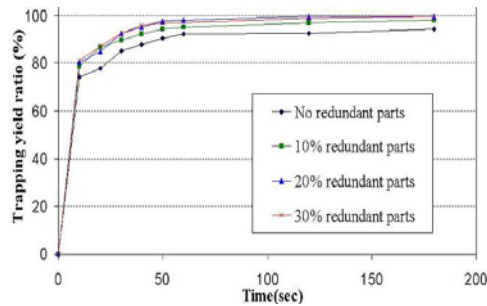


**Fig. 9:** Trapping yield ratios without and with 10-30% part redundancy.

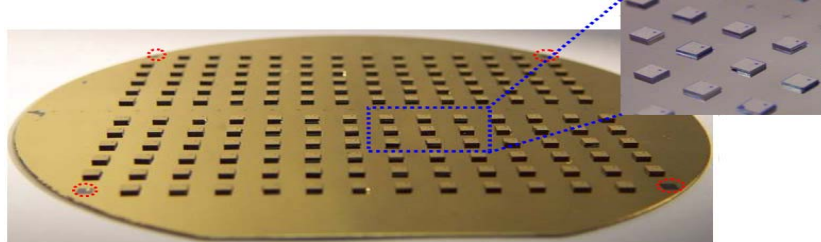


**Fig. 10:** 164 2mm square parts self-assembly on a 4-inch ALT (4 corner receptor sites are blocked by a Petri dish defining moving space for the parts).

### Method II (*a dry process*)

1mm square silicon parts with double pegs are used for this demonstration. Each silicon part has two types of pegs: a CP and an XP on one face. This dry feeding method does not rely on hydrophobic or hydrophilic property of surfaces, so theoretically no surface treatment is required for parts. In the experiments, Au is deposited on the part's flat face opposite to the peg just for high color contrast or better viewing, and a hole in the Au marked the position of the CP or part polarity.

Bulk parts are first uniquely face-oriented on a 4-inch orbitally shaken face-orienting substrate (FOS). The FOS has an array of  $1\text{cm} \times 1\text{cm} \times 240\mu\text{m}$  wells (Fig. 11a). Bulk parts are poured into these wells with approximately uniform distribution. When orbital shaking speed is about 200RPM, our experiments have shown that more than 98% of parts rest on their flat Au faces because tilted parts on their pegs are flipped

over by the combination of collision impact by neighboring parts and centrifugal forces from orbital shaking. The remained tilted parts usually are kept immobile by surrounding parts.

Then these uniquely face-oriented parts are transferred onto a 4-inch ALT. We place the ALT with receptor sites towards the parts onto the FOS, and then turn over the sandwiched structure. When the FOS is removed, more than 99% of parts are palletized onto the ALT except few parts sticking to the FOS.

Finally parts are distributed to receptor sites in one-to-one mode. The part distributing technique is the same as Method I: the CPs are anchored to the CTs. One-to-one registration is also guaranteed by limiting the CT diameter. Trapping yields of  $\sim 98\%$  are achieved with 50% part redundancy in about 10 minutes for each of two 4-inch ALTs having respectively 397 and 720 receptor sites (Fig. 11).

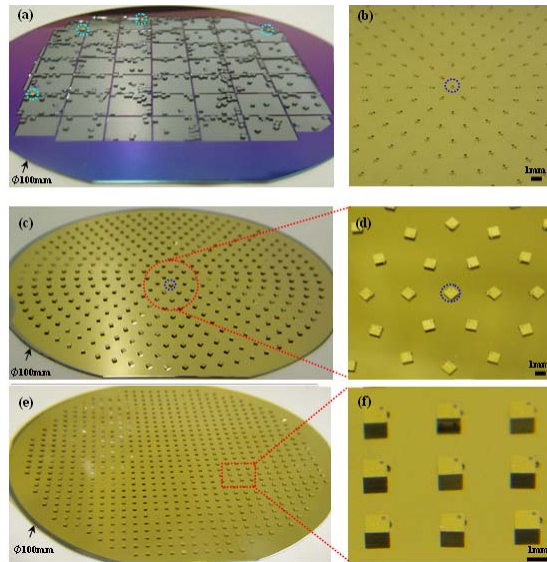


**Fig. 11:** Optical photographs of templates and assembly results. (a) After 1 minute of orbital shaking, only 4 silicon parts stay resting on their peg faces on the  $\Phi 100\text{mm}$  FOS. (b) A partial view of an ALT with a polar array of receptor sites. (c) 388 silicon parts assembled on the  $\Phi 100\text{mm}$  ALT with a polar array of 397 receptor sites. (d) Zoom-in view of the center of the ALT. (e) 710 silicon parts assembled on the  $\Phi 100\text{mm}$  ALT with an orthogonal array of 720 receptor sites. (f) Zoom-in view of a  $3 \times 3$  section of the array of receptor sites.

## 4.2 Part Alignment

Unique alignment is achieved for single- and double-peg parts respectively by gravity-driven alignment and two-stage shape recognition. In our experiments, the gravity-driven alignment is rather rough (maximum rotational misalignment observed is  $18^\circ$ ) because of three factors: (1) the difference between radii of the CP and the CT (they are designed to be concentric when a part is exactly aligned); (2) surface friction; (3) roughly controlled tilt orientation of the ALT. We greatly reduce the misalignment by adding a capillary-driven self-alignment process. Water is introduced to the ALT and part surfaces by steam condensation: steam forms droplet-wise condensation on

hydrophobic surfaces such as the receptor site background, and film-wise condensation on hydrophilic surfaces such as the part sidewall. Water on the part sidewall enters the gap under each part, and then each part is aligned with high accuracy to minimize interfacial energy. Finally water is evaporated by heating. Alignment accuracy of the double-peg-directed assembly is determined by the clearance between the XP and XT (Fig. 12), which is 20 $\mu$ m in our demonstrated results.

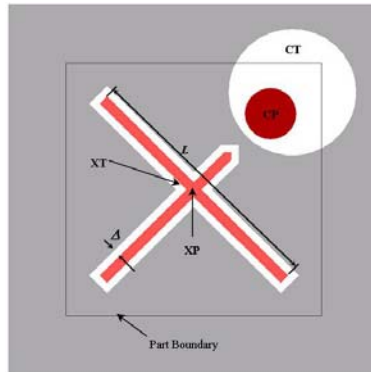


**Fig. 12:** Schematic top view of the exact alignment between a part and a receptor site. The clearance between the XP and XT determines maximum alignment error.

### 4.3 Part Bonding

We propose wafer level flip-chip bonding, a well established process in the IC industry, as the last step to assemble micro flat components by the feature-directed self-assembly processes. The bonding scheme is shown in Fig. 12: interconnect pads are placed on the top flat faces of parts, and all the aligned parts can be transferred to a chip carrier template (CCT) via solder bumps (Fig. 13) on the CCT or a layer of anisotropic conductive film (ACF).

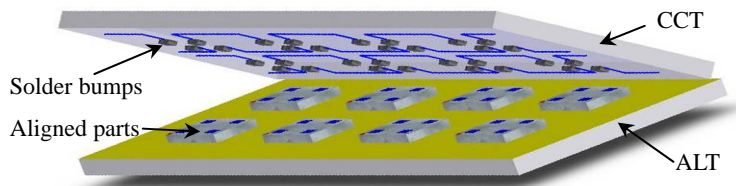


**Fig. 13:** A schematic diagram showing the wafer level flip-chip bonding to transfer aligned parts from the ALT to a CCT.

### 4.4 Multi-batch Assembly

Multi-batch assembly of different types of components can be achieved by multiple transfers using wafer level flip-chip bonding. If alignment features of different components are the same, then an ALT can be repeatedly used for multi-batch assembly. Each time a different batch of components is transferred, and the CCT should be shifted by a certain distance corresponding to the offset from the previous batch (supposing the

ALT is placed in a fixed position with fixed in-plane orientation). As for components of different thickness, the order of assembly should be from the thinnest to the thickest components. In addition, the multiple-transferring technique can also stack several layers of components.

## 5. Conclusions and Discussions

We have demonstrated several capillary-driven self-assembly processes. Depending on the hydrophilic or hydrophobic property of receptor sites, capillary-driven self-assembly can proceed in air or water. Capillary-driven self-alignment is a fast process with high accuracy down to sub microns. In-air and in-water self-assembly processes are demonstrated respectively by assembling PZT actuators and LED components. This PZT self-assembly technique has several major advantages over the conventional bonding method with silver epoxy: accurate placement with self-alignment, tilt free bonding, controllable adhesive thickness, lower process temperatures and high process repeatability. As for the in-water self-assembly, an electrochemical process selectively removing SAM from Au receptor sites enables multi-batch self-assembly of different types of components. Both of the capillary-driven self-assembly processes have two major limitations: (1) random part feeding brings each face of a part the same opportunity to be captured by an acrylate-based adhesive or water droplet on a stationary assembly substrate, although the strength of attraction between the part and the droplet depends on hydrophilicity of the wetted part face; (2) there is no unique alignment for parts with rotational symmetries, such as rectangular parts which are very common for micro components due to widely used straight mechanical dicing. A possible solution to overcome the first limitation is agitating the assembly substrate appropriately to de-bond parts attached by wrong faces and with weaker attraction to adhesive droplets.

In addition to assembling flat components, capillary forces are also exploited for patterning of nano-structures [12]. Hydrophilic receptor sites with hydrophobic background are lithographically patterned, and colloidal aggregation takes place at the center of these receptor sites when water evaporates, leaving behind aggregates of nano-structures with varying morphology: they can reproduce the design of the receptor sites, or reduce their shapes significantly; they can appear, e.g., as monolayers, or as densely packed three-dimensional arrays.

Two types of feature-directed self-assembly processes have also been demonstrated: the single- and double-peg-directed self-assembly processes are respectively based on gravity-driven self-alignment and two-stage shape recognition. Bulk parts are first uniquely face-oriented on either an orbitally shaken water surface or substrate, and then palletized with face-orientation preserved onto 4-inch alignment templates via a hydrophobic carrier wafer or a face-orienting substrate. Finally orbital shaking assists trapping and unique aligning of parts by providing a uniform centrifugal force field. A completely dry assembly process by two-stage shape recognition benefits assembly of components with either movable microstructures or coatings sensitive to aqueous environments, because surface tension of liquid residue from a wet assembly process can deform or break these microstructures. Both of the feature-directed self-assembly processes enable wafer level packaging of micro components without constraints on shape or material. Multiple wafer level transfer processes of uniquely aligned parts to form stacks can be extended to build some simple three-dimensional microstructures.

## Acknowledgments

The research was supported by the following funding sources: NSF career award ECS-9875367, NIH Center of Excellence in Genomic Science and Technology grant 1-P50-HG002360-01, DARPA DSO award FA9550-04-1-0257 and a gift from Microsoft Research. Karl Böhringer was supported in part by a fellowship from the Japan Society for the Promotion of Science. Part of the fabrication was accomplished at the Washington Technology Center at the University of Washington. We would like to thank Fred Forster, Yael Hanein, Chris Morris, Tai-Chang Chen and Brian Williams for helpful discussions and suggestions, and thank the University of Washington MEMS laboratory group members for helpful comments and discussions.

## References

- [1] H. O. Jacobs, A. R. Tao, A. Schwartz, D. H. Gracias, G. M. Whitesides, "Fabrication of Cylindrical Display by Patterned Assembly," *Science*, vol. 296, pp. 323, 2002.
- [2] U. Srinivasan, D. Liepmann, R. T. Howe, "Microstructure to Substrate Self-Assembly Using Capillary Forces," *J. Microelectromechanical Systems*, vol. 10, pp. 17, 2001.
- [3] H. J. Yeh, J. S. Smith, "Fluidic self-assembly for the integration of gas light-emitting diodes on Si substrates," *IEEE Photonics Technology Letters*, vol. 6, pp. 706-708, 1994.
- [4] X. Xiong, Y. Hanein, J. Fang, Y. Wang, W. Wang, D. T. Schwartz, K. F. Böhringer, "Controlled Multi-Batch Self-Assembly of Micro Devices," *ASME/IEEE Journal of Microelectromechanical Systems*, vol. 12, pp. 117-127, 2003.
- [5] S. Liang, X. Xiong, K. F. Böhringer, "Towards Optimal Designs for Self-alignment in Surface-tension Driven Micro-assembly," *IEEE Conference on Micro Electro Mechanical Systems (MEMS)*, Maastricht, Holland, January, 2004.
- [6] J. Fang, K. Wang, K. F. Böhringer, "Self-assembly of Micro Pumps with High Uniformity in Performance," *Solid State Sensor, Actuator, and Microsystems Workshop (Hilton Head'04)*, Hilton Head Island, SC, June 6-10, 2004.
- [7] J. Fang, K. F. Böhringer, "High Yield Batch Packaging of Micro Devices with Uniquely Orienting Self-assembly," *IEEE Conference on Micro Electro Mechanical Systems (MEMS)*, Miami Beach, FL, January 30 - February 3, 2005.
- [8] J. Fang, K. F. Böhringer, "Uniquely Orienting Dry Micro Assembly by Two-Stage Shape Recognition," *The 13th International Conference on Solid-State Sensors, Actuators and Microsystems (Transducers'05)*, Seoul, Korea, June 5-9 (Accepted), 2005.
- [9] K. F. Böhringer, U. Srinivasan, R. T. Howe, "Modeling of capillary forces and binding sites for fluidic self-assembly," *IEEE Conference on Micro Electro Mechanical Systems (MEMS)*, 2001.
- [10] S. Liang, K. Wang, K. F. Böhringer, "Self-assembly of MEMS Components in Air Assisted by Diaphragm Agitation," *IEEE Conference on Micro Electro Mechanical Systems (MEMS)*, Miami Beach, FL, January 30 - February 3, 2005.
- [11] A. J. Bard, L. R. Faulkner, *Electrochemical Methods: Fundamentals and Applications*, 1st ed. New York: Wiley, 1980.
- [12] X. Xiong, K. Wang, K. F. Böhringer, "From Micro-Patterns to Nano-Structures by Controllable Colloidal Aggregation at Air-Water Interface," *IEEE Conference on Micro Electro Mechanical Systems (MEMS)*, Maastricht, Holland, January, 2004.